

Rapid magnitude estimation of great earthquakes for tsunami warning

KATSUMATA, Akio^{1*}, AOKI, Shigeki¹, YOSHIDA, Yasuhiro¹, UENO, Hiroshi¹, Yasuhiro Kaida², Takashi Yokota¹

¹Meteorological Research Institute, JMA, ²OYO Corporation

One of major problems in the tsunami warning for the 2011 off the Pacific coast of Tohoku Earthquake (Mw 9.0) was a lack of awareness of underestimation of the earthquake magnitude at the time soon after the occurrence. Displacement magnitude, which is usually used for the first tsunami warning a few minutes after the earthquake occurrence, could not evaluate such large magnitude due to short cutoff period (six seconds) compared to the rupture duration (about three minutes). Seismic moment could not be determined from the regional seismological network data due to over range of broadband sensor outputs, and it took longer time to estimate it from global data. To overcome these difficulties in earthquake magnitude estimation, we are developing several methods to estimate proper magnitude roughly and to understand possible magnitude underestimation soon after such large earthquakes.

Large earthquakes cause strong shaking in a wide area. Length of strong-shaking area is related to earthquake magnitude. Seismic intensity distribution in Japan can be known in a few minutes after earthquake occurrence owing to a dense on-line network of seismic intensity meter in Japan. The area of seismic intensity greater or equal to 5-upper (the Japan Meteorological Agency seismic intensity scale) reached about 700 kilometers in length. It is possible to estimate earthquake magnitude and source area roughly from the span of strong shaking.

Strong motion is observed at sites close to the source region. Maximum distance between the observation site and source area can be estimated from observed seismic intensity. If source area is assumed on the plate boundary, the fault plane could be estimated. However, the far edge of the fault is not able to be obtained from seismic intensity distribution.

The duration of the strong motion becomes also longer for larger earthquakes. Good correlation is seen between strong-motion duration and earthquake magnitude. The duration of the earthquake in March, 2011 exceeded eighty seconds, which is the largest among those of large earthquakes in and around Japan.

It takes a long time to complete a rupture of a large earthquake. Excitation of long-period seismic wave is one of features of large earthquakes. The cutoff period for the displacement magnitude was too short for the earthquake. Usage of long period components of seismic wave would help to estimate earthquake magnitude properly. A method of watching growth of magnitude from long-period seismic wave was developed. The magnitude from long-period seismic wave was estimated to reach the final value within three minutes for the earthquake in March, 2011.

Combination of these methods is expected to help us to issue a proper tsunami warning for the next great earthquake.

Keywords: magnitude determination, great earthquakes, area of strong motion, strong-motion duration

Rapid estimation of moment tensors for large earthquakes

ASANO, Youichi^{1*}, KIMURA, Hisanori¹

¹National Research Institute for Earth Science and Disaster Prevention

We have developed a method for estimating centroid moment tensor. In order to estimate it from shorter seismograms than those for the routine method in the NIED F-net and AQUA system (Matsumura et al., 2006) assuming point source and impulsive source time function, synthetic seismograms were calculated taking a simplified source time function with a duration time into consideration. We have analyzed seismograms of the 2011 Tohoku earthquake (05:46:17, March 11, 2011 in UTC) recorded by strong motion seismographs of the NIED F-net. These seismograms at 15 stations from 05:44 to 05:52 were applied by a band-pass filter (pass-band: 0.005 ~ 0.02 Hz) and inverted to estimate a moment tensor by a similar algorithm to the AQUA system with grid-searching for duration time and peak time of source time function. Time window for this inversion was selected to be 300 s from the origin time. As a result, we obtained a best model with a 60-s duration time, a peak time of 05:47:33, and Mw 8.8 under a variance reduction of 75 %, which is better than 63 % for impulsive source time function (duration time = 0 s). We have also tried to estimate the moment tensor of the same earthquake from shorter seismograms at six stations from 05:44 to 05:49. Time window for inversion was selected to be 120 s from the origin time. This result shows weak constraint for duration time; however, the estimated Mw was in a range between 8.6 (for duration time = 0 s) and 8.8 (for duration time = 60 s). Seismograms for this analysis at these six stations located in epicentral distances between 140 km and 310 km may include information of peak moment rate and half duration of the source time function. Consequently, we successfully estimated the Mw from these short seismograms.

Keywords: moment tensor, centroid moment tensor

Effects of rupture process in the source inversion of 2011 off the Pacific coast of Tohoku Earthquake Tsunami

TAKAGAWA, Tomohiro^{1*}, Takashi TOMITA¹

¹Port and Airport Research Institute

The 2011 off the Pacific coast of Tohoku Earthquake (Mw 9.0) and Tsunamis attacked and severely damaged the east coast of Japan. Inverse analysis on the tsunami source was conducted on the basis of sea-level observation of GPS buoys and water pressure gauges located near the source area. Observed data are inverted to determine the initial sea-surface height distribution and its time development that are generated by the rupture motion of inter-plate faults and the related sea-floor deformations. We use an inversion method of synthesizing tsunami Green's functions. To compute the Green's functions, tsunami wave propagation was calculated on the basis of the finite-difference approximation of linear long-wave equations in a spherical coordinate system. Such inversions are usually ill-posed problem mainly because of limited observation. To avoid the ill-posedness, smoothing and rupture constrains are imposed. The rupture constraint is based on a priori information about the tsunami source region. The region at a given time is estimated by the distance from epicenter and a rupture velocity. According to the seismic wave analysis by Japan Meteorology Agency, epicenter is located at N38°6.2', E142°51.6', 24 km deep and the rupture velocity and the rupture duration is assumed as 2.0 km/sec and 3 minutes respectively. The inversion result shows that the peak of surface elevation moved eastward from epicenter for first 1 minute to reach close to the Japan Trench and moved northward along the trench axis for next two minutes. The maximum elevation of tsunami source is +6.9 m in total and is located at northeast of epicenter in the west side of the trench axis. The crest of initial wave form is distributed in the west side of the trench. To investigate the effect of rupture process, we perform another inversion with the assumption of rupture velocity as infinity. A major difference between the two inversions is the location of the wave form crest. In the infinite rupture velocity case, the crest penetrates into east side of the trench. The tsunami source model of finite rupture velocity show a better accuracy for the prediction of waveforms which were temporally and/or spatially different from waveforms used in the source inversion. Therefore, it is concluded that the effect of rupture time lag is not negligible in the 2011 off the Pacific coast of Tohoku Tsunami case and the effect should be included in the validation of inundation or damage on the coastal area and the assessment for future risk.

Keywords: 2011 off the Pacific coast of Tohoku Earthquake, tsunami source inversion, rupture process

Effect of offshore tsunami station array configuration on accuracy of near-field tsunami forecast

TSUSHIMA, Hiroaki^{1*}, HIRATA, Kenji¹, HAYASHI, Yutaka¹, MAEDA, Kenji¹, OZAKI, Tomoaki²

¹Meteorological Research Institute, ²Japan Meteorological Agency

1. Introduction

Tsunami forecast based on offshore tsunami data is effective to adequately update tsunami warnings. Several methods have been proposed by recent studies (e.g., Baba et al., 2004; Titov et al., 2005; Tsushima et al., 2009; Hayashi, 2010). Tsushima et al. (2011) applied the tFISH algorithm (Tsushima et al., 2009) retrospectively to the offshore tsunami data from the 2011 Tohoku earthquake, and showed that tFISH is able to contribute to improvement of the forecasts for the coastal sites in the Sanriku region, northern Honshu where many offshore stations were operated at the time of the 2011 Tohoku event. They pointed out that poor azimuthal coverage of offshore stations should degrade forecasts at some coastal sites where no offshore station is located in somewhere along tsunami ray paths to there. In this study, we discuss how an array configuration of offshore tsunami stations affects coastal tsunami forecasts provided by tFISH.

2. Simulation Procedure for Forecasting Tsunami

As a test case, we simulated tsunami forecast of the 2011 Tohoku earthquake. The simulation was carried out as follows: (1) Tsunami waveforms, computed for observation points by assuming a fault model, were regarded as the observed tsunami waveforms. (2) Coastal tsunami waveforms were then estimated from offshore tsunami data by using tFISH. (3) The results of the tsunami forecast were evaluated by comparing the observed waveforms at coastal sites (100 m in water depth) with the predictions from Hokkaido to Kanto.

For calculation of the observed waveforms, we assumed the fault model of Fujii et al. (2011). In the tFISH algorithm, offshore tsunami waveform data are inverted for initial sea-surface height distribution in source region, and then prediction of coastal tsunami waveforms are synthesized by using the estimated height and pre-computed tsunami Green functions.

We here assumed three different array configurations. First consists of the cabled OBPG and GPS buoy stations that were operated during the 2011 Tohoku earthquake, called the existed array configuration. Second consists of the existed array and three additional OBPG stations that are supposed to locate on the inner slope of the Japan Trench, called the IT array configuration. These stations are distributed from off Aomori to off Fukushima with a spacing of ~200 km nearly parallel to the trench. Third consists of the existed array and three additional OBPG stations that are supposed to locate on the outer part of the Japan Trench, called the OT array configuration.

3. Results

We forecasted coastal tsunami waveforms at 20 min after the mainshock using the observed tsunami data at offshore stations in each configuration. In the case of the existed array configuration, the first peaks of the tsunamis were observed at the two OBPG stations, resulting in a good agreement between the observed and the predicted waveforms at the coastal points near Miyako and Kamaishi. At the other coastal points, however, predicted tsunami amplitudes were halves of the observations. In the case of the IT array configuration, the forecasting results improved dramatically. At the time of 20 min after the event, the pressure variation due to the coseismic seafloor deformation appears on the records at two additional IT array stations. We consider that in this case four offshore OBPG data constrained the source strongly, which make tsunami forecasts accurate. Similar improvements were found in the results for the OT array case. The additional OBPG stations are located far from the source, but the most part of the first tsunami wave was observed there until 20 min after the event because the almost all path run much deep ocean. The present results indicate that when strong tsunami energy were observed at offshore stations, the forecasting accuracy would be improved greatly, even though offshore station was not located between a source region and a coastal point where tsunami should be forecasted.

Keywords: real-time tsunami forecasting, near-field tsunami, ocean bottom pressure gauge, GPS buoy, DART

Issues specific to offshore tsunami observation in near-field

HIRATA, Kenji^{1*}, Hiroaki TSUSHIMA¹

¹Meteorological Research Institute

The March 11 Tohoku earthquake (M9.0) destroyed vast coastal zone of the northern Japan together with many coastal tide gauges. It also did offshore tsunami observation stations off Tohoku. A part of them, like GPS tsunami buoys, was already recovered but the others are not. In 2011, JMA and MEXT started their plans to construct new offshore tsunami observation networks off Tohoku. When these networks will be built up once, it is possible that the offshore data, which will be transmitted to the land on real-time base, may improve the reliability of the regional forecast for near-field tsunamis. However, there seem to be issues to be overcome for achieving precise near-field tsunami forecast. We would like to discuss two of them below.

First issue is pressure resolution in ocean-bottom pressure gauge (OBPG). When a large earthquake occurs, offshore ocean-bottom pressure gauges (OBPG) usually record tsunami and preceding pressure fluctuations with frequencies much shorter than the period of the tsunami. The pressure fluctuations are primarily attributed to seismic Rayleigh waves traveling through oceanic lithosphere from a distant earthquake (Fillioux, 1982). In some cases, such pressure fluctuation masks tsunami signals for nearby earthquakes (Okada, 1995; Tsushima et al., 2009). In the 2003 Tokachi-oki earthquake (Mw8.0), however, a pressure signal with an amplitude of a few hundreds of kPa (equivalent to several tens of meters H₂O) was observed with the near-field OBPGs, while tsunami amplitude was estimated only an order of a few kPa (equivalent to only a few tens of centimeters H₂O). The period of the main energy of the observed pressure signals was several seconds that are much shorter than tsunami period. In addition, the tsunami and pressure signals were completely overlapped. The large pressure signals observed is considered mostly low-frequency hydroacoustic waves reverberating between the sea surface and ocean bottom through water layer, which was theoretically predicted by Kajiura (1970), and these are closely related to ocean-bottom vertical motion due to an earthquake (Matsumoto and Mikada, 2005; Nosov et al., 2007) and remain mostly in the source region (Nosov, 2000). The near-field experience in 2003 suggests that to extract tsunami information precisely from OBPG records for coastal tsunami forecast, we will have to observe ocean-bottom pressure in much wider range of amplitude from an order of millimeters H₂O to an order of, at least, several tens of meters H₂O and in much broader frequency range from an order of 0.1 seconds to an hour. Pressure resolution of OBPGs attached on the existing Japanese cabled observatories is not so fine to satisfy the above conditions. In near-future, near-field OBPG measurement will require finer pressure resolution than the present.

Second issue is sudden temperature change on deep ocean floor. In the 2003 Tokachi-oki earthquake, we found that the temperature within OBPGs in the source region suddenly decreased by an order of 0.1 degree C per ten minutes, which was much rapid change in the deep ocean floor environment off Tokachi (Hirata et al., 2003). Such sudden change in temperature caused artificial pressure signal that distort tsunami waveforms owing to a transient thermal response of OBPGs (Takahasi, 1983; Hirata and Baba, 2006). The mechanism of such sudden temperature change remains unresolved so that we cannot decide whether this is local phenomena or not. Any near-field tsunami forecast based on records monitored with OBPGs, experienced a sudden temperature change, may include not small prediction error unless the transient thermal effect of OBPGs is properly corrected.

Keywords: tsunami, offshore, observation, tsunami forecast

Early warning system with GPS-TEC observation

KAMOGAWA, Masashi^{1*}, KAKINAMI, Yoshihiro²

¹Dpt. of Phys., Tokyo Gakugei Univ., ²Institute of Seismology and Volcanology, Hokkaido University

Traveling ionospheric disturbances generated by an epicentral ground/sea surface motion, ionospheric disturbances associated with Rayleigh-waves as well as post-seismic 4-minute monophasic atmospheric resonances and other-period atmospheric oscillations have been observed in large earthquakes. In addition, a giant tsunami after the subduction earthquake produces an ionospheric hole which is widely a sudden depletion of ionospheric total electron content (TEC) in the hundred kilometer scale and lasts for a few tens of minutes. The tsunamigenic ionospheric hole detected by the TEC measurement with Global Position System (GPS) was found only in huge subduction earthquakes. This occurs because plasma is descending at the lower thermosphere where the recombination of ions and electrons is high through the meter-scale downwelling of sea surface at the tsunami source area, and is highly depleted due to the chemical processes. The results imply that magnitude of the tsunamigenic ionospheric hole is related to that of the tsunami. It means that we can directly observe the tsunami several minutes after the subduction earthquake occurs.

Keywords: Early warning system, Tsunamigenic ionospheric disturbance, GPS

Quantitative Analysis of Magnetic Signals induced by the 2011 Tohoku Tsunami Flow around Chichijima Island(Part 2).

TATEHATA, Hideo^{1*}, Yozo Hamano²

¹JMA, ²IFREE JAMSTEC

Magnetic field generated by the 2011 off the Pacific Coast of Tohoku Earthquake Tsunami (March 11) was observed at the Chichijima geomagnetic observation station. Significantly at first, the onset of the geomagnetic perturbation precedes the tsunami observation at Chichijima tide gauge (Futami observation station) by 20 minutes. In order to interpret this phenomena, we constructed a numerical model has 10*10 grids spacing 100km around Chichijima island, and estimates the sea water flow and height at each grid. These tsunami data were also estimated the influence to the geomagnetism according to Hamano model (Hamano et al., 2011).

Comparing the results to the geomagnetic observation, the preceding geomagnetic perturbation is considered that it was induced by the earliest arrival tsunami waves at north-west offshore area of the island. And it is also shown that the geomagnetic observation can detect tsunami waves in wide area comparing to the tsunami observation by tide gauge. But we could say that the simulation results were not sufficient, because 10*10 grids might not be enough for induced magnetic field by tsunami waves.

At this lecture, we will show the enough results using 100*100 grids spacing 2km. Moreover, we will show the simulated induced magnetic field by the fictitious geomagnetic observatory at the coast of Iwate and Miyagi prefectures where damaged by the 2011 Tsunamis. These results could have the meaning to the disaster prevention. Although the magnetic observation at coast has disadvantage for tsunami detection, because of shallow water depth around the station does not have A strong excitation magnetic field. However, this method or equipment does not need to soak in the sea water, the observation method using generated magnetic field can observe tsunami waves even from hill on land. Therefore, it may be able to continue observation when tide gauge stations will be destroyed by huge tsunamis. It will be shown the simulated results in this case.

Keywords: tsunami, geomagnetic field, motional induction, Chichijima, Kakioka, Faraday's Law

Tsunami source estimation of the 2011 Tohoku-oki earthquake (M9.0) and its foreshock (M7.3) using ocean bottom magnetic

ICHIHARA, Hiroshi^{1*}, HAMANO, Yozo¹, BABA, Kiyoshi², KASAYA, Takafumi¹

¹Japan Agency for Marine-Earth Science and Technology, ²Earthquake Research Institute, University of Tokyo

The electromagnetic induction theory predicts that motion of conductive seawater in the geomagnetic field induces variation of electromagnetic fields as known as dynamo effect. Thus electromagnetic observation is expected to be a novel tsunami meter that can detect propagated direction of tsunamis in addition to the sea level change (e.g. Toh et al., 2011). When the 2011 Tohoku-oki earthquake (M9.0, March 11) occurred, an ocean bottom electromagnetometer (here after OBEM) settled near the Japan Trench (39.0N latitude, 144.8E longitude, 5830m deep) clearly recorded tsunami induced magnetic signals.

The variations in the magnetic field after the main shock show a unipolar impulsive wave for a short duration (about 4 min) in all three components. The vertical magnetic field indicates the tsunami travel time to the OBEM station (4 minutes from the initial rupture). Amplitude of the vertical impulse (15 nT) corresponds to 2.3 m of sea level change. In addition, the horizontal magnetic field components indicate propagated direction of tsunami to the OBEM station (WNW). Based on this information, the tsunami source of the main shock was determined along the Japan Trench but at about 100 km north from main rupture zone of the main shock (around 39.0-39.5N latitude, 144.8E longitude). Joint analysis of OBEM data and offshore sea-level gage data (GPS gages and deep pressure gages) supports this location and constrained the tsunami source to a narrow east-west area (<30 km in width). On the other hand, the tsunami induced vertical magnetic signal associated with the foreshock was detected after 10 minutes from the rupture initiation. Based on the back propagation curves of the arrival time of tsunami to the OBEM station and the offshore sea-level stations, the tsunami source of the fore shock was determined around 38.4N latitude and about 80km west from the Japan trench, almost same location of the epicenter. Thus the estimated tsunami sources of the fore and main shocks are quite different although the epicenters of main and fore shocks are determined in the almost same location. In addition, elastic fault models are hard to explain observed tsunami waveforms by the main shock including OBEM data although it can explain observed tsunami waveforms by the fore shock. They imply different source mechanism of these tsunamis and thus detailed study of the tsunami source model is required especially for the main shock.

Keywords: tsunami electromagnetism, OBEM, 2011 Tohoku-oki earthquake

3-D simulations of tsunami generation using an unstructured mesh FEM: investigation of the 2011 Tohoku-Oki Earthquake

OISHI, Yusuke^{1*}, Matthew D. Piggott², MAEDA, Takuto³, Stephan C. Kramer², Gareth S. Collins², TSUSHIMA, Hiroaki⁴, FURUMURA, Takashi³

¹Fujitsu Laboratories of Europe Ltd., ²Imperial College London, ³CIDIR/ERI, The University of Tokyo, ⁴Meteorological Research Institute

For a detailed investigation of tsunami generation processes caused by fault motion in a large earthquake, a three-dimensional tsunami generation and propagation simulation approach using an unstructured mesh finite element method is proposed. The present method is applied to the 2011 off the Pacific coast of Tohoku Earthquake (M9.0) and the validity of the method is tested.

In simulations of tsunamis resulting from earthquakes, the sea bottom deformation is calculated from faulting parameters, using for example the equations of Okada (1985), and the free surface deformation is often assumed to equal this. However, this assumption is not always true. When the timescales for the bottom deformation are large, when the horizontal spatial scales of the deformation are small, or when the water depth is large, the free surface deformation tends to be smaller than the bottom deformation. For example, Saito and Furumura (2009) quantitatively evaluated this 'filtering' effect. One of their conclusions was that the filtering effect is important when the horizontal scale of the deformation is smaller than ten times the water depth, in the case of a short deformation timescale.

In the 2011 Tohoku Earthquake, it is indicated that a large slip in a shallow part of the crust caused short wavelength tsunami waves (e.g. Fujii et al., 2011; Maeda et al., 2011). To properly deal with this kind of short wavelength initial water height distribution, it is necessary to take account of the difference between the bottom and free surface deformations induced by the filtering effect.

An analytical solution based upon an approximation is sometimes used to calculate the free surface deformation from the bottom deformation to take into account the filtering effect (e.g. Takahashi, 1942; Kajiura, 1963). The effect can be modeled realistically by solving the full 3-D equations without any approximation (e.g. Takahashi and Furumura, 2009). However, the computational cost of solving the 3-D equations in a wide source region like the 2011 Tohoku earthquake is very large. Therefore, in this study, the 3-D incompressible Navier-Stokes equations are solved using an unstructured mesh finite element method, which can efficiently refine the mesh and hence position computational degrees of freedom at points to maximize accuracy and minimize computational expense. The unstructured mesh also enables accurate reproduction of the complex bathymetry near the trench. In the simulations, the bottom deformation is imposed as an inflow boundary condition for velocity, which is caused by the movement of the sea water just above the sea bottom (Saito and Furumura, 2009). In the vertical direction, the nodes should be placed so that the sea bottom boundary layer and the vertical velocity and pressure profiles are efficiently resolved.

In this presentation, a comparison between analytical solutions from linear potential theory and the simulation results, an application of the present method to the 2011 Tohoku earthquake generated tsunami, and the computational performance including the parallel efficiency will be reported.

Keywords: unstructured mesh, finite element method, tsunami, simulation, the 2011 off the Pacific coast of Tohoku Earthquake

Tsunami prediction of Japanese Island based on numerical simulations

MIYOSHI, Takayuki^{1*}, SAITO, Tatsuhiko¹

¹NIED

We have investigated tsunamis generating along the coast of Japanese Island by a numerical simulation. Tsunami simulations are based on a linear shallow-water wave equation. We assumed 200 sources around Japanese Island and evaluated tsunamis at stations located every about 20 km along the coastlines. The initial tsunami height is assumed ellipsoid-shape. We calculated initial travel times of tsunami and travel times of maximum tsunami height on the stations from every source, and then we made tsunami information maps. We compared the results and observations in order to examine the validity of the simulations. Based on a distribution of initial tsunami height shown by Saito et al. (2011), our results well explain observations of the 2011 Tohoku giant tsunami.

Acknowledgements: We used the tsunami observation data reported by Japan Metrological Agency.

Keywords: tsunami, numerical simulation, travel time, initial tsunami height, maximum tsunami height

Tsunami heights of the North Sanriku-Oki earthquake of August 23rd, 1856

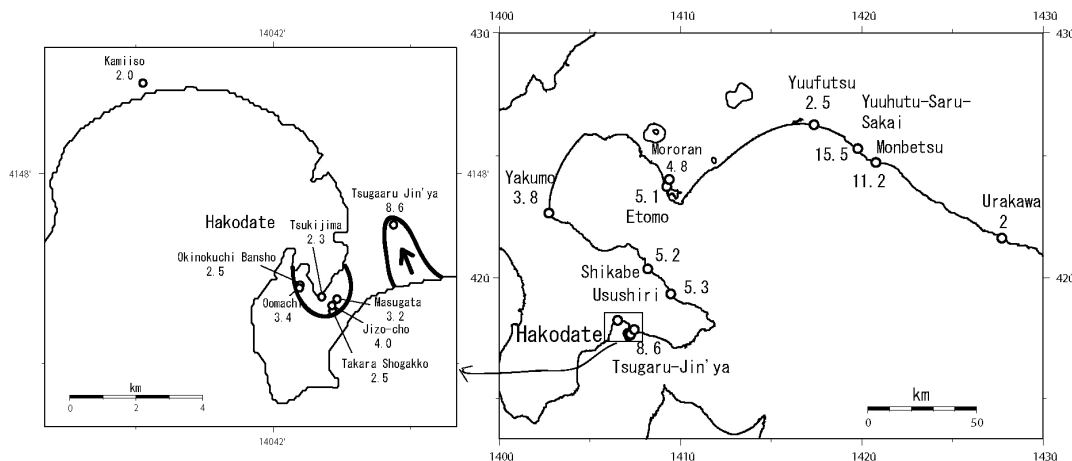
TSUJI, Yoshinobu^{1*}, IMAI, Kentaro², Horie, Takehito³, NONOYAMA, Kosuke³, IWABUCHU, Yoko⁴, IMAMURA, Fumihiko², Yoshino, Masahumi³

¹none, ²Tohoku Univ., ³Alfa Hydraulic Engineering Co., ⁴JNES

A large earthquake (M7.5) occurred off the north Sanriku coast on August 23rd, 1856. A remarkable tsunami accompanied with the earthquake hit the Pacific coasts of north part of the Japanese Islands. The epicentral area is estimated nearly the same as that of the 1968 Tokachi Oki Earthquake. In the present study we conducted field surveys along the coast of Hokkaido, including Hakodate and Muroran cities. Hakodate was one of the two open port to foreign countries at that time, and the consulate office of Russia had been founded. From three days before the main shock, foreshocks were felt twice or three times a day at Hakodate. The main shock occurred at 13 o'clock and the tsunami hit the port of Hakodate at around 15 o'clock. Sea level rose up about three meters and invaded into streets up to the streets about 300 meters from the west coast. Sea water invaded into the mansion of Tsugaru clum from the east coast up to the height of 8.6 meters above the sea level.

The total distribution of the tsunami height is shown in the figure.

Keywords: the 1856 North Sanriku Earthquake, historical tsunami, historical earthquake, tsunami in Hokkaido, tsunami at Hakodate



Atmospheric boundary waves excited by the tsunami generation - the great Sumatra-Andaman Islands Earthquake in 2004 -

IWAKUNI, Makiko^{1*}, ARAI, Nobuo¹, IMANISHI, Yuichi², WATADA, Shingo², Takuma Oi³, MURAYAMA, Takahiko¹, NOGAMI, Mami¹

¹Japan Weather Association, ²Earthquake Research Institute, University of Tokyo, ³Toho Mercantile CO., LTD

The sudden and strong vertical displacements of ocean surface are known to be the source of the long-period acoustic-gravity waves including the boundary waves in the atmosphere. Arai et al. (2011) observed atmospheric pressure changes caused by the tsunami generation of the 2011 Off the Pacific Coast of Tohoku earthquake, and identified them as "atmospheric boundary waves" on the basis of the waveform characteristics. The sudden and strong vertical displacements of ocean surface caused by the Sumatra-Andaman earthquake in 2004 also had produced long-period acoustic-gravity waves (Mikumo et al. 2008).

We re-explore barograph data observed around the source region of the Sumatra earthquake in 2004. Atmospheric pressure changes caused by the ocean uplift and subsidence were detected at 4 IMS (International Monitoring System for CTBT verification regime) stations. IMS stations provide two kinds of data, one is the band pass filtered (0.02-4Hz) output and the other is the absolute pressure output. Band pass filtered data are archived and used for CTBT's monitoring purpose. Absolute pressure data are not archived at all IMS stations. If the absolute data is not available, the band pass filtered data have been corrected by deconvolving the filter response and original records have been restored.

Long-period atmospheric pressure disturbance signals which were excited by uplift and subsidence related to the tsunami generation were observed at IS52 (Diego Garcia), IS33 (Madagascar), IS32 (Kenya) and IS35 (Namibia). The pressure signals were identified as atmospheric boundary waves based on their characteristics.

Earth orbiter "Jason-1" measures ocean surface topography. When the tsunami caused by the earthquake had been propagating through the Indian Ocean, Jason-1 flew over the propagating area. Jason-1 detected the two propagating tsunami wave fronts as the elevated ocean surface topography which indicates two isolated peaks. Detected atmospheric boundary waves also have the same characteristics. Atmospheric boundary waves retain the initial shape of the tsunami, because they are little dispersive. Observed signals suggest the Sumatra-Andaman earthquake had two isolated tsunami source regions.

Keywords: Atmospheric boundary wave, Tsunami source, International Monitoring System